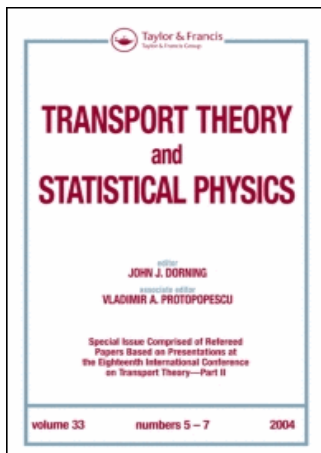


This article was downloaded by:[HEAL- Link Consortium]  
On: 24 October 2007  
Access Details: [subscription number 772810551]  
Publisher: Taylor & Francis  
Informa Ltd Registered in England and Wales Registered Number: 1072954  
Registered office: Mortimer House, 37-41 Mortimer Street, London W1T 3JH, UK



## Transport Theory and Statistical Physics

Publication details, including instructions for authors and subscription information:  
<http://www.informaworld.com/smpp/title~content=t713597305>

### Formulation and Stability Analysis of Rapidly Convergent Iteration Schemes for the 2-D Linearized BGK Equation

J. Lihnaropoulos<sup>a</sup>; S. Naris<sup>a</sup>; D. Valougeorgis<sup>a</sup>

<sup>a</sup> Department of Mechanical and Industrial Engineering, University of Thessaly, Volos, Greece

Online Publication Date: 01 July 2007

To cite this Article: Lihnaropoulos, J., Naris, S. and Valougeorgis, D. (2007) 'Formulation and Stability Analysis of Rapidly Convergent Iteration Schemes for the 2-D Linearized BGK Equation', *Transport Theory and Statistical Physics*, 36:4, 513 -

528

To link to this article: DOI: 10.1080/00411450701468415

URL: <http://dx.doi.org/10.1080/00411450701468415>

PLEASE SCROLL DOWN FOR ARTICLE

Full terms and conditions of use: <http://www.informaworld.com/terms-and-conditions-of-access.pdf>

This article maybe used for research, teaching and private study purposes. Any substantial or systematic reproduction, re-distribution, re-selling, loan or sub-licensing, systematic supply or distribution in any form to anyone is expressly forbidden.

The publisher does not give any warranty express or implied or make any representation that the contents will be complete or accurate or up to date. The accuracy of any instructions, formulae and drug doses should be independently verified with primary sources. The publisher shall not be liable for any loss, actions, claims, proceedings, demand or costs or damages whatsoever or howsoever caused arising directly or indirectly in connection with or arising out of the use of this material.

## FORMULATION AND STABILITY ANALYSIS OF RAPIDLY CONVERGENT ITERATION SCHEMES FOR THE 2-D LINEARIZED BGK EQUATION

J. LIHNAROPOULOS, S. NARIS, and D. VALOUGEORGIS

Department of Mechanical and Industrial Engineering, University  
 of Thessaly, Volos, Greece

*Various  $H_N$  rapidly convergent schemes are proposed to speed up the slow convergence of the iterative solution of 2-D linearized Bhatnagar-Gross-Krook (BGK) kinetic equation containing up to the first moments of the distribution function. The formulation of the 2-D  $H_N$  acceleration schemes is provided in a generalized manner, followed by a formal 2-D Fourier-mode stability analysis to determine the most efficient  $H_N$  approach. The  $H_0$  method is the most efficient when the kinetic equation contains only the zeroth moment of the distribution function, while when it contains the zeroth and the first moments the most efficient approach is the  $H_1$ . Although the analysis and the conclusions are restricted to the continuous form of the equations, they are indicative for the associated discrete equations.*

**Keywords:** Kinetic, Discrete velocities, Iteration, Acceleration

### 1. Introduction

The efficient and accurate solution of multidimensional linear kinetic equations has attracted a lot of attention during the last few years, mainly due to these equations' application in the rapidly evolving technological fields of micro-electromechanical systems and nanotechnology (Gad-el-Hak 2002). It is well known that rarefied flows, which traditionally are tackled via kinetic theory (Cercignani 1988), are identical to nano- and micro-flows (Karniadakis and Beskok 2002). One of the important advantages of applying kinetic theory, compared to

---

Received 17 October 2005, Revised 9 May 2006, Accepted 9 June 2006

Address correspondence to D. Valougeorgis, Department of Mechanical and Industrial Engineering, University of Thessaly, Pedion Areos, Volos 39334, Greece. Tel.: 00302421074058; Fax: 00302421074050; E-mail: diva@mie.uth.gr

other approaches, is the fact that this methodology is applicable to the whole range of gas rarefaction. Consequently, the results are obtained in a unified manner and are valid from the free molecular through the transition up to the continuum regimes.

One of the most common numerical techniques for solving linearized steady-state kinetic equations is the implementation of a simple iteration scheme between the distribution function and the macroscopic quantities, which are defined as moments of the distribution function (Valougeorgis 1988; Sharipov and Seleznev 1998). This iterative computation has a very close resemblance with the so-called source iteration (SI) scheme applied to steady-state neutron and radiative discrete ordinates calculations (Lewis and Miller 1984). In steady-state kinetic theory the unknown distribution is a function of six independent variables: the three spatial variables and the three components of the molecular velocity vector. Hence, since these calculations involve the replacement of the continuum spectrum of molecular velocities by an appropriately chosen finite set of discrete velocities, they are called, instead of *discrete ordinates*, *discrete velocity calculations* (Cercignani 1988; Sharipov and Seleznev 1998).

Over the years, the discrete velocity method has been successfully applied to solve various steady-state linear kinetic model equations describing different types of flow problems in the field of rarefied gas dynamics. However, it is well known to researchers involved in discrete velocity computations of stationary kinetic equations that while the convergence of the iteration scheme works well in the free molecular regime, it degrades as we march into the transition regime and becomes unacceptably slow as we approach the continuum regime. Due to this computational pitfall, in many cases the applicability of the kinetic methodology has been limited up to certain gas rarefaction, and beyond that limit a continuum-type approach based on the well-known conservative hydrodynamic equations is implemented. This is a serious drawback, since the main advantage of mesoscale kinetic-type approaches is their ability to deduce results valid in the whole range of the gas rarefaction.

The convergence of the iterative map of the discrete velocity calculations applied in steady-state kinetic calculations has been recently studied via a typical Fourier stability analysis, and its slow convergence has been justified (Valougeorgis and Naris 2003).

In the same work, rapidly convergent iteration methods, similar (but not identical) to the synthetic-type acceleration schemes in neutron and radiative transport (Lewis and Miller 1976; Adams and Larsen 2002; Valougeorgis et al. 1988), have been proposed. Since they are developed by taking Hermitian moments of the kinetic equations, they are called  $H_N$  iteration schemes. The efficiency of these novel rapidly convergent methods has been also confirmed computationally (experimentally) by solving several rarefied gas dynamics problems (Valougeorgis and Naris 2003; Naris et al. 2004). However, the theoretical part of this work has been focused mainly on 1-D kinetic equations, while the experimental part has been applied to 2-D kinetic equations, which, however, include only the zeroth-order moment of the distribution function.

Here, we investigate the 2-D linearized Bhatnagar-Gross-Krook (BGK) kinetic equation containing the zeroth and the first moments of the distribution function covering from a technological point of view wider range of applications. Various 2-D  $H_N$  acceleration schemes are proposed, and their formulation is provided in a generalized manner. In addition, a formal 2-D Fourier-mode stability analysis is performed to determine the most efficient  $H_N$  approach. Certain aspects of previous work are included for completeness and comparison purposes. Our analysis and therefore our conclusions are limited to the continuous form of the equations. However, previous experience with similar acceleration schemes in neutron and radiative transport (Valougeorgis et al. 1988), as well as more recent work in kinetic theory (Valougeorgis and Naris 2003) clearly indicate that the present obtained results are directly applicable to the associated discretized equations.

## 2. Kinetic Equations under Investigation

Following a well-known projection procedure of the linearized BGK equation, we obtain the 2-D kinetic equation

$$\begin{aligned} \mu \frac{\partial f^{(l+1/2)}}{\partial x} + \eta \frac{\partial f^{(l+1/2)}}{\partial y} + \delta f^{(l+1/2)}(x, y, \mu, \eta) \\ = \delta \left[ F_{0,0}^{(l)}(x, y) + A(\mu F_{1,0}^{(l)}(x, y) + \eta F_{0,1}^{(l)}(x, y)) \right] + S(x, y) \end{aligned} \quad (1)$$

and the double integral expression of the moments

$$F_{m,n}^{(l+1)}(x, y) = \frac{1}{\pi} \int_{-\infty}^{\infty} \int_{-\infty}^{\infty} H_m(\mu) H_n(\eta) f^{(l+1/2)}(x, y, \mu, \eta) e^{-\mu^2 - \eta^2} d\mu d\eta. \quad (2)$$

In (1) and (2),  $f(x, y, \mu, \eta)$  is the unknown distribution function;  $x$  and  $y$  are the spatial independent variables;  $\mu$  and  $\eta$  are the independent variables related to the  $x$  and  $y$  components of the microscopic velocity vector;  $H_m$  and  $H_n$  denote the Hermite polynomials of order  $m$  and  $n$  respectively;  $F_{m,n}(x, y)$ , with  $m + n \leq 1$ , are the zeroth and the first two Hermitian moments of the distribution function;  $S(x, y)$  is a source term; and  $\delta \in [0, \infty)$  is the rarefaction parameter. For  $\delta = 0$ , the flow is free molecular, while as  $\delta \rightarrow \infty$  the flow is approaching the continuum (hydrodynamic) limit. Our objective is to solve (1) and (2) in a computationally efficient manner in the whole range of the rarefaction parameter  $\delta$ . The constant  $A$  takes the values of  $A = 0$  or  $A = 1$ . When  $A = 0$ , (1) describes incompressible gas flow in a duct of arbitrary cross section. The flow is in the longitudinal direction, which is vertical to the  $x$ - $y$  plane, due to imposed pressure and temperature gradients parallel to the flow (Valougeorgis and Naris 2003; Naris et al. 2004; Naris et al. 2005). When  $A = 1$ , (1) describes compressible gas flow in a cavity (Naris and Valougeorgis 2005), or in a grooved channel (Karniadakis and Beskok 2002), or through a thin slit connecting two vessels (Cercignani and Sharipov 1992; Sharipov 1996). In this case the flow may be boundary driven or due to imposed pressure and temperature gradients on the  $x$ - $y$  plane. It is seen that (1) and (2) may be used to model several flow configurations.

Finally the superscript ( $l$ ) denotes the iteration index of the iteration map applied to the typical discrete velocity algorithm. We denote this nonaccelerated iterative scheme by the acronym *DVM*.

It is obvious that (1), with  $A = 0$  or  $A = 1$ , looks qualitatively similar to the neutron or radiative transport equation with isotropic and linearly anisotropic scattering, respectively.

Of course, here, instead of the Legendre polynomials, the moments are given in terms of the Hermite polynomials.

### 3. Formulation of Accelerated Schemes

The first synthetic-type acceleration schemes in the area of kinetic theory and rarefied gas dynamics have been presented in Valougeorgis and Naris (2003). Then, this approach has been applied successfully to speed up the slow convergence rate of the DVM iteration scheme in several incompressible gas flow problems in channels and ducts. In all cases the main kinetic equations were similar to (1) with  $A = 0$ . The proposed schemes have the same characteristics with the  $P_N$  schemes in neutron and radiative transport (Lewis and Miller 1976; Adams and Larsen 2002). They are based on the formulation of moment equations, which are solved coupled with the kinetic equations. The moment equations are formulated by taking Hermitian moments of the kinetic equations. Various schemes may be defined depending upon the number of accelerated moments.

In 1-D problems, the  $H_N$  acceleration scheme consists of the kinetic equations; the  $N + 1$  moment equations, which accelerate (starting from the zeroth moment) the first  $N$  moments; and the integral expression for the  $N + 1$  nonaccelerated moment. Thus as we increase the order of the acceleration scheme by one, only one additional moment equation is added in the set of the accelerated equations.

In 2-D problems, although the methodology remains, in principle, the same implies a rather cumbersome mathematical manipulation. To derive an  $H_N$  acceleration scheme, (1) is multiplied first by the weighting factor term  $(1/\pi) \exp(-\mu^2 - \eta^2)$  and then successively by all possible combinations of  $H_m(\mu)$   $H_n(\eta)$  such that  $m + n \leq N$ , with  $m, n = 0, 1, \dots, N$ . The resulting equations are integrated over  $\mu$  and  $\eta$  to deduce a set of  $\sum_{i=1}^{N+1} i = 1 + 2 + \dots + (N + 1)$  moment equations, which are solved at each iteration in order to accelerate the first  $\sum_{i=1}^{N+1} i$  moments of order less than or equal to  $N$ . Therefore, these moments are the accelerated moments, while the moments with order higher than  $N$  are estimated by the integral expression (2) and are defined as the nonaccelerated moments.

For a better understanding of the above procedure, we consider the special case of the  $H_1$  iteration scheme. Equation (1) is multiplied first by the weighting factor term  $(1/\pi) \exp(-\mu^2 - \eta^2)$  and then successively by  $H_0(\mu) H_0(\eta)$ ,  $H_1(\mu) H_0(\eta)$ , and  $H_0(\mu) H_1(\eta)$ . The resulting equations are integrated over  $\mu$  and  $\eta$  to yield the following three moment equations:

$$\frac{\partial F_{1,0}^{(l+1)}}{\partial x} + \frac{\partial F_{0,1}^{(l+1)}}{\partial y} = S \quad (3)$$

$$\frac{\partial F_{0,0}^{(l+1)}}{\partial x} + \delta(1-A)F_{1,0}^{(l+1)} = -\frac{1}{2} \left( \frac{\partial F_{2,0}^{(l+1/2)}}{\partial x} + \frac{\partial F_{1,1}^{(l+1/2)}}{\partial y} \right) \quad (4)$$

$$\frac{\partial F_{0,0}^{(l+1)}}{\partial y} + \delta(1-A)F_{0,1}^{(l+1)} = -\frac{1}{2} \left( \frac{\partial F_{1,1}^{(l+1/2)}}{\partial x} + \frac{\partial F_{0,2}^{(l+1/2)}}{\partial y} \right). \quad (5)$$

Equations (3)–(5) are used to accelerate the moments  $F_{0,0}$ ,  $F_{1,0}$ , and  $F_{0,1}$  with order less or equal to  $N = 1$ , while the moments  $F_{2,0}$ ,  $F_{1,1}$ , and  $F_{0,2}$  with order higher than  $N = 1$ , are estimated by the integral expression

$$F_{m,n}^{(l+1/2)}(x, y) = \frac{1}{\pi} \int_{-\infty}^{\infty} \int_{-\infty}^{\infty} H_m(\mu) H_n(\eta) f^{(l+1/2)}(x, y, \mu, \eta) e^{-\mu^2 - \eta^2} d\mu d\eta, \quad (6)$$

with  $m, n = 1, 2$  such that  $m + n = 2$ .

This procedure we may generalize for any  $H_N$  iteration scheme, which now will consist of the kinetic equation (1); the accelerated moments

$$\frac{\partial F_{1,0}^{(l+1)}}{\partial x} + \frac{\partial F_{0,1}^{(l+1)}}{\partial y} = S, \quad m = n = 0 \quad (7)$$

$$m \frac{\partial F_{m-1,n}^{(l+1)}}{\partial x} + n \frac{\partial F_{m,n-1}^{(l+1)}}{\partial y} + \delta(1-A)F_{m,n}^{(l+1)} + \frac{1}{2} \left( \frac{\partial F_{m+1,n}^{(l+1)}}{\partial x} + \frac{\partial F_{m,n+1}^{(l+1)}}{\partial y} \right) = 0, \quad m + n = 1 \quad (8)$$

$$\begin{aligned}
m \frac{\partial F_{m-1,n}^{(l+1)}}{\partial x} + n \frac{\partial F_{m,n-1}^{(l+1)}}{\partial y} + \delta F_{m,n}^{(l+1)} \\
+ \frac{1}{2} \left( \frac{\partial F_{m+1,n}^{(l+1)}}{\partial x} + \frac{\partial F_{m,n+1}^{(l+1)}}{\partial y} \right) = 0, \quad 1 < m+n < N
\end{aligned} \tag{9}$$

$$\begin{aligned}
m \frac{\partial F_{m-1,n}^{(l+1)}}{\partial x} + n \frac{\partial F_{m,n-1}^{(l+1)}}{\partial y} + \delta F_{m,n}^{(l+1)} \\
= -\frac{1}{2} \left( \frac{\partial F_{m+1,n}^{(l+1/2)}}{\partial x} + \frac{\partial F_{m,n+1}^{(l+1/2)}}{\partial y} \right); \quad m+n = N
\end{aligned} \tag{10}$$

and the nonaccelerated moments

$$\begin{aligned}
F_{m,n}^{(l+1/2)}(x, y) = \frac{1}{\pi} \int_{-\infty}^{\infty} \int_{-\infty}^{\infty} H_m(\mu) H_n(\eta) f^{(l+1/2)} \\
(x, y, \mu, \eta) e^{-\mu^2 - \eta^2} d\mu d\eta, \quad m+n = N+1.
\end{aligned} \tag{11}$$

More specifically, the  $H_N$  accelerated iteration scheme works as follows:

1. From (1), after we assume its right-hand side, we compute  $f(x, y, \mu, \eta)$ .
2. From (11), we integrate  $f$  to find the nonaccelerated moments  $F_{m,n}^{(l+1/2)}(x, y)$ , with  $m+n = N+1$ .
3. From the system (7)–(10), we find the accelerated moments  $F_{m,n}^{(l+1)}(x, y)$ , with  $m+n \leq N$ .
4. The first three accelerated moments are substituted on the right-hand side of (1), and the iteration procedure is continued upon convergence.

Equations (7)–(11) have been written in a generalized manner, which describes the formulation of any  $H_N$  iteration scheme for either  $A = 0$  or  $A = 1$ .

It is seen that in the 2-D case, as we increase the order of the acceleration scheme, the number of moment equations, which are added in the set of the accelerated equations, is significantly



increased. Therefore, it is important to keep the order of the acceleration scheme as low as possible. For example, an  $H_3$  iteration scheme will include (1); 10 moment equations defined by (7)–(10), with  $m + n \leq 3$ ; and five nonaccelerated moments defined by (11), with  $m + n = 4$ . It is noted, however, that in general, although the computational effort per iteration is increased, the number of required iterations and the overall CPU time are drastically decreased.

#### 4. Stability Analysis

To quantitatively describe the performance of the typical DVM and the proposed  $H_N$  iteration schemes, we consider a simple homogeneous infinite medium problem ( $-\infty < x, y < \infty$ ). In (1) and (2), we set  $S(x, y) = 0$  and interpret the functions  $f$  and  $F_{m,n}$  as iteration errors. We consider a single Fourier error mode and set

$$f(x, y, \mu, \eta)^{(l+1/2)} = \omega^l g(\mu, \eta) \exp[i\lambda(\theta_x x + \theta_y y)], \quad (i = \sqrt{-1}), \quad (12)$$

and

$$\begin{aligned} F_{m,n}(x, y)^{(l+1)} &= \omega F_{m,n}(x, y)^{(l)} = \dots = \omega^{l+1} F_{m,n}(x, y)^{(0)} \\ &= \omega^{l+1} b_{m,n} \exp[i\lambda(\theta_x x + \theta_y y)] \end{aligned} \quad (13)$$

where  $\omega(\lambda)$  is the eigenvalue corresponding to the Fourier wave-number  $\lambda = \lambda(\theta_x, \theta_y)$ , with  $\theta_x^2 + \theta_y^2 = 1$ . Substituting (12) into (1), we obtain the eigenfunction

$$g(\mu, \eta) = \frac{b_{00} + A(b_{10}\mu + b_{01}\eta)}{1 + i(\lambda/\delta)(\theta_x\mu + \theta_y\eta)}. \quad (14)$$

In addition, in order to proceed with the mathematical manipulation, we define the auxiliary integrals

$$G_{mn}(x, y) = \frac{1}{\pi} \int_{-\infty}^{\infty} \int_{-\infty}^{\infty} H_m(\mu) H_n(\eta) g(x, y, \mu, \eta) e^{-\mu^2 - \eta^2} d\mu d\eta \quad (15)$$

and

$$\Lambda_{2k} = \frac{1}{\sqrt{\pi}} \int_{-\infty}^{\infty} \frac{x^{2k}}{1 + ((\lambda/\delta)x)^2} \exp[-x^2] dx, \quad k = 0, 1, \dots \quad (16)$$

We start by studying the convergence rate of the nonaccelerated DVM scheme. The Fourier ansatz (12) and (13) are substituted at the right- and left- hand side, respectively, of (2). When  $A = 0$ , we find the scalar equation

$$\omega_{DVM} b_{00} = G_{00}, \quad (17)$$

which after some routine manipulation yields the eigenvalue

$$\omega_{DVM} = \Lambda_0. \quad (18)$$

When  $A = 1$ , we obtain the system

$$\begin{aligned} \omega b_{00} &= G_{00} \\ \omega b_{10} &= G_{10} \\ \omega b_{01} &= G_{01}, \end{aligned} \quad (19)$$

which is solved as an eigenvalue problem to deduce the three eigenvalues

$$\omega_{DVM}^{(1)} = \Lambda_0 \quad (20)$$

and

$$\omega_{DVM}^{(2,3)} = \frac{1}{2} \left[ (\Lambda_0 + 2\Lambda_2) \pm \sqrt{(\Lambda_0 + 2\Lambda_2)^2 - 8\Lambda_2} \right]. \quad (21)$$

It is seen that the expression for the first eigenvalue given by (20) is identical to the corresponding one for  $A = 0$  (Equation 18), while the other two are in complex conjugates. Plots of the eigenvalues versus  $\lambda/\delta$  for the DVM scheme are given in Figure 1. For  $\omega_{DVM}^{(2,3)}$  we plot their absolute values. In all cases the maximum absolute value of  $\omega$ , which defines the spectral radius of the iteration map, occurs at  $\lambda = 0$  and is equal to 1. Hence, in real computations, although the flat mode  $\lambda = 0$  is not present, the DVM iteration scheme will be arbitrarily slow. In addition, it is evident from Figure 1 that as we are approaching the continuum regime and the rarefaction parameter  $\delta \rightarrow \infty$ ,

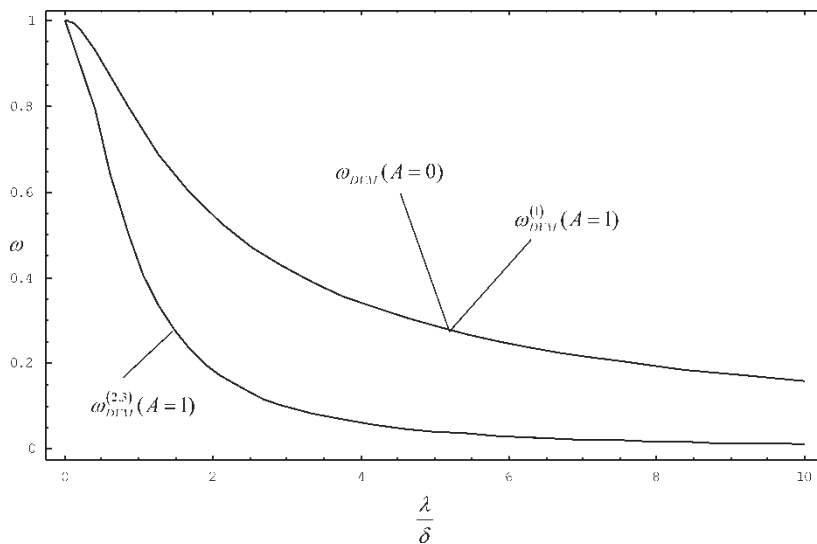


**FIGURE 1** Plots of  $\omega$  versus  $\lambda/\delta$  for the DVM iteration scheme with  $A = 0$  and  $A = 1$ .

the convergence rate of the DVM will degrade, since now, the ratio  $(\lambda/\delta) \rightarrow 0$  even for  $\lambda \gg 0$ .

Next we study the convergence of the  $H_0$  iteration scheme, which may be considered as a special case since the procedure for developing this scheme is different than the generalized procedure presented in Section 3. The methodology is similar to the diffusion synthetic acceleration (DSA) iteration scheme in discrete ordinates calculations (Adams and Larsen 2002). In particular, (4) and (5) are differentiated with respect to  $x$  and  $y$  respectively, and then they are added. Finally, (3), with  $S(x, y) = 0$ , is substituted into the resulting equation to deduce an acceleration equation for the zeroth-order moment of the form

$$\frac{\partial^2 F_{0,0}^{(l+1)}}{\partial x^2} + \frac{\partial^2 F_{0,0}^{(l+1)}}{\partial y^2} = -\frac{1}{2} \left( \frac{\partial^2 F_{2,0}^{(l+1/2)}}{\partial x^2} + 2 \frac{\partial^2 F_{1,1}^{(l+1/2)}}{\partial x \partial y} + \frac{\partial^2 F_{0,2}^{(l+1/2)}}{\partial y^2} \right). \tag{22}$$

Equation (22) is known as the diffusion equation. For the case  $A = 0$ , the stability analysis applied to (1), (2), and (22) results

in the scalar equation

$$\omega_{H_0} b_{00} = -\frac{1}{2}(\theta_x^2 G_{20} + 2\theta_x \theta_y G_{11} + \theta_y^2 G_{02}). \quad (23)$$

The double integrals on the right-hand side are properly combined to give the eigenvalue

$$\omega_{H_0} = \Lambda_0 - 2\Lambda_2. \quad (24)$$

For the case  $A = 1$ , the zeroth moment is accelerated by (22), while the first two nonaccelerated moments are defined by (2) with the pairs  $(m = 0, n = 1)$  and  $(n = 0, m = 1)$ . Thus, we obtain the system

$$\begin{aligned} \omega b_{00} &= -\frac{1}{2}(\theta_x^2 G_{20} + 2\theta_x \theta_y G_{11} + \theta_y^2 G_{02}) \\ \omega b_{10} &= G_{10} \\ \omega b_{01} &= G_{01}, \end{aligned} \quad (25)$$

which again is formulated as an eigenvalue problem to yield  $\omega_{H_0}^{(1)} = 0$  and

$$\omega_{H_0}^{(2)} = \omega_{H_0}^{(3)} = \Lambda_0. \quad (26)$$

It is noted that the expressions (24) and (26) for the eigenvalues corresponding to  $A = 0$  and  $A = 1$ , respectively, are different. Their behavior in terms of  $\lambda/\delta$  is shown in Figure 2. It is seen that when the  $H_0$  iteration scheme is applied to the kinetic equation with  $A = 0$ , the convergence rate of the iteration map is rapidly improved. In this case the theoretical spectral radius of the  $H_0$  iteration scheme, shown in Table 1, is equal to 0.320. However, when  $A = 1$ , as is obvious from (26), there is no improvement, and the spectral radius remains equal to 1.

We continue with the investigation of the convergence rates of higher-order  $H_N$  iteration schemes. We have found that for  $H_N$  iteration schemes, with  $N \geq 1$ , we always obtain one dominant eigenvalue, while all the remaining ones are identically equal to zero. In addition, when  $N \geq 1$ , both the  $A = 0$  and  $A = 1$  cases reduce to exactly the same results, which now depend only on the order  $N$  of the method. Hence, each  $H_N$  acceleration method, with  $N \geq 1$ , applied to the kinetic

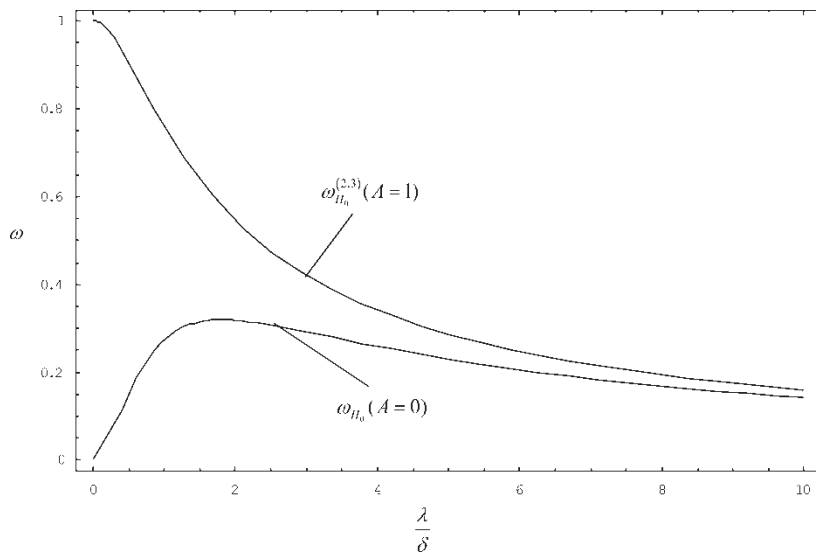


**FIGURE 2** Plots of  $\omega$  versus  $\lambda/\delta$  for the  $H_0$  iteration scheme with  $A = 0$  and  $A = 1$ .

Equation (1) with  $A = 0$  or  $A = 1$ , performs equally well or poorly. It is concluded that in general an  $H_N$  iteration scheme, with an order  $N$  equal to or larger than the maximum order of the moments on the right-hand side of the kinetic equation, which in our case is equal to 1, sets all eigenvalues except one equal to zero. Thus, estimation of the one nonzero eigenvalue is adequate to obtain the convergence rate of the accelerated iteration scheme.

**TABLE 1** Spectral radius of the DVM and  $H_N$ , with  $N = 0, 1, 2, 3$ , iteration schemes for  $A = 0$  and  $A = 1$

Iteration scheme	Spectral radius	
	$A = 0$	$A = 1$
DVM		1.00
$H_0$	0.320	1.00
$H_1$		0.320
$H_2$		2.00
$H_3$		0.211

We have examined in detail the  $H_1$ ,  $H_2$ , and  $H_3$  iteration schemes. After some routine mathematical manipulation, we find in terms of the  $G_{mn}$  integrals given by (15) the following expressions for the nonzero eigenvalues of the  $H_1$ ,  $H_2$ , and  $H_3$  iteration schemes, respectively:

$$\omega_{H_1} b_{00} = -\frac{1}{2}(\theta_x^2 G_{20} + 2\theta_x \theta_y G_{11} + \theta_y^2 G_{02}) \quad (27)$$

$$\omega_{H_1} b_{00} = \frac{1}{4}i\left(\frac{\lambda}{\delta}\right)(\theta_x^3 G_{30} + 3\theta_x^2 \theta_y G_{21} + 3\theta_x \theta_y^2 G_{12} + \theta_y^3 G_{03}) \quad (28)$$

$$\omega_{H_3} b_{00} = \frac{1}{4}\left(\frac{1}{3 + 2(\lambda/\delta)^2}\right)(\theta_x^4 G_{40} + 4\theta_x^3 \theta_y G_{31} + 6\theta_x^2 \theta_y^2 G_{22} + 4\theta_x \theta_y^3 G_{13} + \theta_y^4 G_{04}). \quad (29)$$

Applying a coordinate rotation, the right-hand sides of (27)–(29), which are given in terms of the double integrals  $G_{mn}$ , may be expressed in terms of the single integrals  $\Lambda_{2k}$ , given by (16). This is achieved by introducing the new variables

$$\begin{pmatrix} \mu' \\ \eta' \end{pmatrix} = \begin{pmatrix} \theta_x & \theta_y \\ -\theta_y & \theta_x \end{pmatrix} \begin{pmatrix} \mu \\ \eta \end{pmatrix} \quad \text{and} \quad \begin{pmatrix} b'_{10} \\ b'_{01} \end{pmatrix} = \begin{pmatrix} \theta_x & \theta_y \\ -\theta_y & \theta_x \end{pmatrix} \begin{pmatrix} b_{10} \\ b_{01} \end{pmatrix} \quad (30)$$

with

$$\begin{pmatrix} \mu & \eta \end{pmatrix} \begin{pmatrix} b_{10} \\ b_{01} \end{pmatrix} = \begin{pmatrix} \mu' & \eta' \end{pmatrix} \begin{pmatrix} b'_{10} \\ b'_{01} \end{pmatrix} \quad (31)$$

and taking into account that the Jacobian of the transformation is equal to 1. Then, we obtain the analytical expressions

$$\omega_{H_1} = \Lambda_0 - 2\Lambda_2, \quad (32)$$

$$\omega_{H_2} = \left(\frac{\lambda}{\delta}\right)^2 (2\Lambda_4 - 3\Lambda_2), \quad (33)$$

and

$$\omega_{H_3} = \frac{1}{3 + 2(\lambda/\delta)^2} (4\Lambda_4 - 12\Lambda_2 + 3\Lambda_0) \quad (34)$$

for the eigenvalues of the  $H_1$ ,  $H_2$ , and  $H_3$  iteration schemes, respectively. It is noted that these results are identical to the corresponding ones in slab geometry. Since, as expected, in the absence of discretization all multidimensional  $H_N$  iteration schemes behave exactly like the corresponding 1-D schemes, it may be stated that the formulation of the 2-D  $H_N$  schemes and their stability analysis is correct. It is noted that for  $A = 0$  the expressions (24) and (32) for the eigenvalues  $\omega$  of the  $H_0$  and  $H_1$  schemes, respectively, are identical.

Plots describing the behavior of the eigenvalues (32)–(34) versus  $\lambda/\delta$  are shown in Figure 3, while the spectral radius of the iteration maps are provided in Table 1. It is concluded that the  $H_1$  and  $H_3$  iteration schemes both for  $A = 0$  and  $A = 1$ , as well as the  $H_0$  scheme for  $A = 0$  (see Figure 2), efficiently suppress the error modes that have strong and weak spatial and angular dependence. The latter are the ones that are not efficiently suppressed by the DVM for  $A = 0$  and  $A = 1$  and by the  $H_0$  scheme for  $A = 1$ . It is also obvious that the efficiency of the  $H_1$  and  $H_3$  methods and of the  $H_0$  scheme for  $A = 0$  (from Figures 2 and 3)

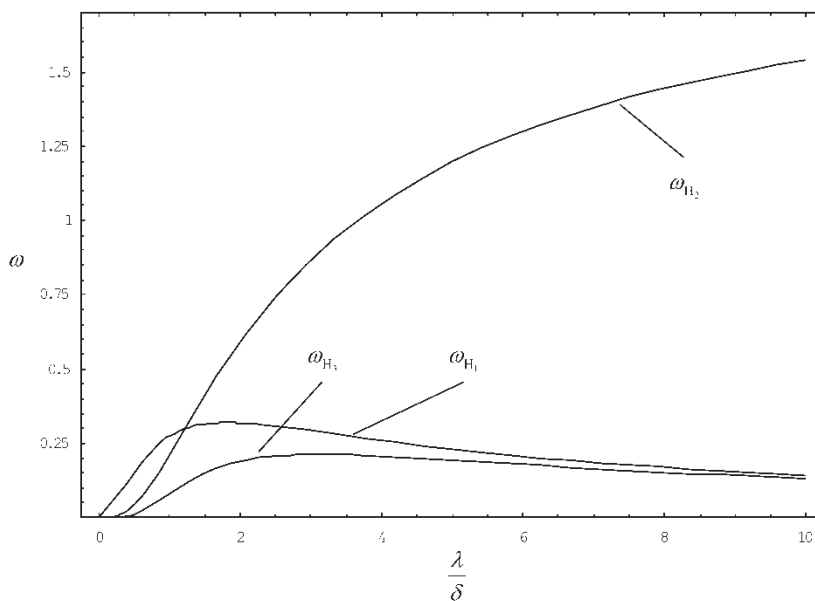


**FIGURE 3** Plots of  $\omega$  versus  $\lambda/\delta$  for the  $H_1$ ,  $H_2$ , and  $H_3$  iteration schemes with  $A = 0$  and  $A = 1$ .

does not degrade as the rarefaction parameter  $\delta \rightarrow \infty$ . The performance of the  $H_2$  scheme in all cases is very poor. Its spectral radius is equal to 2, and it is even worse than the DVM scheme, although it requires much more computational effort per iteration. Finally, taking into account the spectral radius of the  $H_0$ ,  $H_1$ , and  $H_3$  iteration schemes, shown in Table 1, and the associated computational effort per iteration for each scheme, it is reasonable to conclude that the  $H_0$  method is the most efficient when the kinetic equation contains only the zeroth moment of the distribution function ( $A = 0$ ), while when it contains the zeroth and the first moments ( $A = 1$ ) the most efficient approach is the  $H_1$ .

## 5. Concluding Remarks

The objective of the present work is to speed up the slow convergence of the iterative solution of 2-D linearized kinetic equations containing up to the first moments of the distribution function. This is achieved by formulating synthetic-type  $H_N$  rapidly convergent schemes. The spectral radii of these methods are estimated by a Fourier-mode stability analysis, and the optimum scenarios are determined. It has been shown, as expected, that in the absence of discretization the 2-D  $H_N$  schemes behave exactly like the corresponding ones in slab geometry. A Fourier-mode analysis of the  $H_N$  discrete velocity equations is under way.

## Acknowledgments

The authors take this opportunity to thank Professor E. W. Larsen for several helpful discussions and comments regarding this (and other) work. Partial support by the Association EURATOM—Hellenic Republic (Controlled Thermonuclear Fusion program) and the Greek Ministry of Education (Pythagoras program) is gratefully acknowledged.

## References

- Adams, M. L., Larsen, E. W. (2002). Fast iterative methods for discrete-ordinates particle transport calculations. *Progr. Nucl. Energy* 40(1):3–159.



- Cercignani, C. (1988). *The Boltzmann Equation and Its Applications*. New York: Springer.
- Cercignani, C., Sharipov, F. (1992). Gaseous mixture slit flow at intermediate Knudsen numbers. *Phys. Fluids A* 4(6):1283–1289.
- Gad-el-Hak, M. (2002). *The MEMS Handbook*. Boca Raton, FL: CRC Press.
- Karniadakis, G. E., Beskok, A. (2002). *Micro Flows: Fundamentals and Simulation*. New York: Springer.
- Lewis, E. E., Miller, W. F., Jr. (1976). A comparison of  $P_1$  synthetic acceleration techniques. *Trans. Am. Nucl. Soc.* 23:202–203.
- Lewis, E. E., Miller, W. F., Jr. (1984). *Computational Methods of Neutron Transport*. New York: Wiley.
- Naris, S., Valougeorgis, D. (2005). The driven cavity flow over the whole range of the Knudsen number. *Phys. Fluids* 17(9):907106.1–907106.12.
- Naris, S., Valougeorgis, D., Kalempa, D., Sharipov, F. (2004). Gaseous mixture flow between two parallel plates in the whole range of the gas rarefaction. *Physica A* 336(3–4):294–318.
- Naris, S., Valougeorgis, D., Kalempa, D., Sharipov, F. (2005). Pressure, temperature and density driven micro flows of gas mixtures in rectangular ducts. *Phys. Fluids* 17(10):100607.1–100607.12.
- Naris, S., Valougeorgis, D., Sharipov, F., Kalempa, D. (2004). Discrete velocity modelling of gaseous mixture flows in MEMS. *Superlattices and Microstructures* 35(3–6):629–643.
- Sharipov, F. (1996). Rarefied gas flow through a slit: Influence of the boundary condition. *Phys. Fluids* 8(1):262–268.
- Sharipov, F., Seleznev, V. (1998). Data on internal rarefied gas flows. *J. Phys. Chem. Ref. Data* 27:657–706.
- Valougeorgis, D. (1988). Couette flow of a binary gas mixture. *Phys. Fluids* 31: 521–524.
- Valougeorgis, D., Naris, S. (2003). Acceleration schemes of the discrete velocity method: Gaseous flows in rectangular microchannels. *SIAM J. Sci. Comput.* 25(2):534–552.
- Valougeorgis, D., Williams, M., Larsen, E. (1988). Stability analysis of synthetic acceleration methods with anisotropic scattering. *Nucl. Sci. Eng.* 99:91–98.